SIMULATION OF CONTRAST ENHANCED LITHOGRAPHY

by

Richard A. Ferguson

Memorandum No. UCB/ERL M87/42

16 June 1987

SIMULATION OF CONTRAST ENHANCED LITHOGRAPHY

by

Richard A. Ferguson

Memorandum No. UCB/ERL M87/42

16 June 1987

ELECTRONICS RESEARCH LABORATORY

College of Engineering
University of California, Berkeley
94720

SIMULATION OF CONTRAST ENHANCED LITHOGRAPHY

by

Richard A. Ferguson

Memorandum No. UCB/ERL M87/42

16 June 1987

ELECTRONICS RESEARCH LABORATORY

College of Engineering
University of California, Berkeley
94720

Simulation of Contrast Enhanced Lithography

Richard A. Ferguson

ABSTRACT

The SAMPLE program has been modified to include contrast enhanced lithography. The contrast enhancement material (CEM) and the underlying photoresist are bleached simultaneously to include coupled exposure effects. The CEM is modeled using Dill's model for positive photoresist and a bleachable index of refraction. An energy increment selection routine has been implemented to allow proper convergence for contrast enhanced lithography. An analytical solution to Dill's equations by Babu and Barouch is included for increased speed and reduced storage. The modified program is used to compare several different lithographic techniques to CEM. Simulation shows that the resolution capability and exposure latitude of CEM is superior to single layer photoresists. The CEM and bilayer resist (PCM) processes are equivalent in resolution, linewidth control, and proximity effects both experimentally and in simulation on silicon substrates. Experimentally, however, CEM suffers from a much larger proximity effect than PCM on aluminum substrates which is not seen in simulations. Several factors which are not included in the simulation such as lateral scattering from the substrate and flare may be responsible.

May 22, 1987

Acknowledgements

First, I would like to thank my family, and especially my parents, whose constant love and support have gotten me where I am through the good and the bad. Thanks also to Professor Andy Neureuther for his guidance on this work and for knowing all that needed to be known. Gino Addiego all deserves thanks for his extensive explanations of the SAMPLE program and his suggestions on the direction of this project. I would also like to thank Bill Bell for the use of his plotting program on several of the figures in this report.

This work was supported by industrial contributions from Philips/Signetics and Intel through the California MICRO program, proposal 85-220.

Chapter 1

Introduction

As integrated circuits become more complex and faster speeds are required, device dimensions must be reduced. This continual need for smaller linewidths pushes photolithographic systems closer to their ultimate limits. Increasing the obtainable resolution in photolithography can be achieved either through improvements in the optical imaging system or the photoresist system. Decreasing the wavelength (λ) or increasing the numerical aperture (NA) both improve the resolution of the optical system. Techniques such as multilayer resists, anti-reflection coatings, and contrast enhanced lithography all improve the resolving capabilities of the photoresist system. However, as these methods become both more abundant and complex, their experimental analysis, comparison and optimization become more difficult, time consuming, and expensive. Simulation can be a valuable tool in examining some of these issues. One method for improved resolution, contrast enhanced lithography, has been investigated through simulation with a modified version of the SAMPLE [1] program.

The concept of contrast enhanced lithography [2] and the first contrast enhancement material, or CEM, [3] were introduced at General Electric by Griffing and West in 1983. Later, General Electric released a second material, CEM-420 [4] (the original became CEM-388), for exposures at longer wavelengths. O'Toole [5] fit the bleaching characteristics of CEM to Dill's exposure parameters for positive photoresist and compared the performance of CEM to standard and bilayer resist processes on nonreflecting substrates by modifying SAMPLE. Neureuther et al. [6] also examined the resolution capability of CEM by modifying SAMPLE to obtain the transmitted image for a layer of CEM assuming a nonreflecting substrate. Oldham[7] has examined the CEM in terms of photoresist contrast gain by use of an analytical solution to Dill's equations derived by Babu and Barouch.[8] In their respective studies, both Neureuther et al. and Oldham used their proposed simulations to generate design graphs for the optimization of a CEM process.

In this report, the modifications to the SAMPLE program required for CEM are described in detail. The program allows for simultaneous bleaching of the CEM and the underlying photoresist with reflecting substrates. The model for the exposure of the CEM is based upon Dill's model[9] for positive

photoresist, but also includes an index of refraction that changes as the CEM is exposed. An energy increment selection routine has been implemented for proper convergence when two layers with different material properties are present, as with contrast enhanced lithography. An alternate algorithm for CEM exposure has also been implemented that uses an analytical solution by Babu and Barouch[8] for photoresist exposure on nonreflecting substrates to approximate the initial stages of the CEM exposure. This solution results in faster program speed and less required storage. The program is then used to investigate the capabilities of contrast enhanced lithography. CEM is compared with a standard photoresist process in terms of resolution and linewidth control with changes in exposure. Several other techniques for improving the resolution of the photoresist system such as anti-reflection coatings and bilayer resist processes are also compared with CEM over a variety of processing conditions.

Chapter 2

Overview of Contrast Enhanced Lithography

The contrast of an aerial image for a periodic line and space pattern is defined by:

$$C = \frac{I_{max} - I_{min}}{I_{max} + I_{min}} \tag{2.1}$$

where I_{max} and I_{min} are the maximum and minimum intensities in the image. The contrast is a measure of the quality of the image produced by the imaging system. Each particular photoresist system requires a certain minimum image contrast to resolve the image within a prescribed tolerance. Standard photoresist processes usually require contrasts greater than 0.95. As will be described, contrast enhanced lithography reduces the contrast needed to successfully reproduce an aerial image within the required tolerances.

Contrast enhancement material or CEM is a bleachable layer, typically 0.4 to 0.8 μm, that is spun onto the surface of standard photoresist prior to exposure. As seen from Figure 1,[10] the CEM during exposure is initially opaque, but beyond a certain dose becomes almost completely transparent. This material property results in the low intensity regions of the aerial image taking longer to bleach through the CEM to the underlying photoresist than the high intensity regions. If the dose is selected properly, the high intensity regions of the image will pass through the CEM while the low intensity regions are still being absorbed. Since dose is defined as the integral of intensity, the contrast seen by the underlying photoresist can be defined by:

$$C = \frac{D_{max} - D_{min}}{D_{max} + D_{min}} \tag{2.2}$$

where D_{max} and D_{min} are the maximum and minimum doses reaching the photoresist from the CEM. Since D_{min} has been reduced with respect D_{max} while passing through the CEM, the underlying photoresist will see a higher contrast than that of the incident aerial image. As a result of the CEM increasing the contrast seen by the photoresist, the photoresist system (CEM and photoresist) is able to resolve aerial images of lower contrast than the photoresist is alone. Oldham [7] has shown that contrast enhanced lithography can also be thought of as a method to increase the photoresist system contrast, γ, which is defined as the slope of the photoresist thickness remaining versus the log of the dose.

The CEM process involves several complexities that are not involved in standard photoresist processes. The CEM must be deposited on the photoresist before exposure and removed from the photoresist surface before development. Because some of the incident energy is absorbed in the CEM, the wafer must be exposed with a dose that is typically 2 to 4 times larger than that required for the photoresist alone.

Chapter 3

SAMPLE Modifications for Contrast Enhanced Lithography

3.1 Introduction

The current release of the SAMPLE program, version 1.6a, can simulate the exposure and development of a single layer of photoresist. This version was modified to perform the simultaneous bleaching of a single layer of photoresist beneath a layer of CEM. This chapter describes the modifications required to allow contrast enhanced lithography in SAMPLE.

3.2 CEM Exposure Model

3.2.1 A, B, and C Parameters

Dill's model for exposure of positive photoresist [9] is used to describe the exposure of CEM. The model consists of bleachable and nonbleachable absorption parameters, A and B, and a bleaching rate, C. These parameters can be obtained by curve fitting to experimental measurements of percent transmission versus dose such as Figure 1. References by O'Toole,[5] Griffing et al.,[10] and West et al.[4] were used to obtain parameters for simulation of General Electric's CEM-388 and CEM-420. These values are shown in the Table 3.1 below.

Table 3.1 -- CEM Exposure Parameters

A (μm^{-1})	B (μm^{-1})	C (cm^2/mJ)	Material	λ (nm)	Where
11.99	0.178	0.0786	CEM-388	405	O'Toole
12.00	0.001	0.0640	CEM-388	405	Griffing et al.
7.214	0.157	0.0318	CEM-420	436	West et al.

The first set of parameters was both measured and fitted by O'Toole,[5] while the other two sets of parameters were estimated from curves of percent transmission versus dose given in the listed refer-

ences. Although all the simulations in this report were done at 436 nm, both the second and third sets of parameters were used in these simulations.

3.2.2 Index of Refraction

According to the Kramer-Kronig relations, if either the real or imaginary part of the index of refraction changes, so must the other part. The imaginary part of the index of refraction, or the extinction coefficient, k, is defined by:

$$k = -\frac{(AM + B)\,\lambda}{4\pi} \tag{3.1}$$

where M is the normalized amount of photoactive compound remaining and λ is the exposure wavelength. Since the amount of photoactive compound, M, changes during bleaching, so does the extinction coefficient. For photoresist, however, A is on the order of 0.5 μm^{-1}, which results in a small value of k over the entire range of M. SAMPLE therefore assumes that the real part of the index of refraction, n, is unaffected by exposure. For CEM, however, the A value is typically on the order of 10 μm^{-1} (see Table 3.1). The extinction coefficient is now significant when compared to the real part of the refractive index and will exhibit a large change as M goes from maximum to minimum. Thus, by the Kramer-Kronig relations, a change must result in n as M changes and, therefore, k changes. As of this report, no experimental data is available on the index of refraction as a function of M. A simple linear relationship has been assumed such that:

$$n = n_a M + n_b \tag{3.2}$$

3.3 Bleaching and Development Algorithm Modifications

The exposure of a bleachable material using Dill's model[9] is described by the equations:

$$\frac{\partial I}{\partial x} = -(AM + B)\,I \tag{3.3}$$

$$\frac{\partial M}{\partial t} = -ICt \tag{3.4}$$

where A, B, and C are defined in the previous section, I is the intensity, t is time, and M is the normalized amount of photoactive compound remaining. SAMPLE version 1.6a uses a numerical algorithm by Berning[11] to solve the above equations for a single layer of photoresist. The photoresist is first subdi-

vided into many vertical layers. For each energy increment, the amount of energy absorbed in each photoresist layer is calculated. Using this information, the M values and extinction coefficients are updated in each layer. This continues until the required dose is reached.

To incorporate contrast enhanced lithography, the CEM is also subdivided into layers, assigned the appropriate A, B, and C parameters and indices of refraction, and placed on top of the photoresist layers. The algorithm then proceeds as before. The only difference is that the top layers corresponding to the CEM have different exposure parameters than the underlying layers that correspond to the photoresist. The real part of the index of refraction must also be updated for the CEM layers after each energy increment as described in section 3.2.2. This simultaneous bleaching of both layers incorporates exposure coupling effects between the two layers that would not be included in a routine that first bleaches the CEM and then uses that information to expose the photoresist.

When the exposure is completed, the final result is a matrix that contains the M values for each defined layer. In the standard photoresist process in SAMPLE, these M values are used in the development routine where the final profile is calculated. With the CEM process, only the layers that correspond to the photoresist are needed since the CEM is removed before development. This removal step is implemented by shifting the matrix up by the amount of CEM layers present. After that, all that remains are the photoresist layers which can then be sent to the development routine to obtain the desired profile. Although in this implementation the CEM has no effect on the development, in reality, an induction effect is often seen at the surface of the photoresist. More experimental work is required to successfully model this effect to increase the accuracy of current simulations.

3.4 Energy Increment Selection

For the numerical solution of equations 3.3 and 3.4 to be accurate, the size of the energy increments must be made small enough for proper convergence. When the energy increments become too small, though, computation time and storage become prime concerns. When only one layer of photoresist is present, the selection of the energy increments is relatively simple. However, when two materials of different properties are used, as in contrast enhanced lithography, the selection becomes much more difficult. The problem is made even more difficult by the nonlinear properties of the CEM.

A method is described in the following sections in which the energy increments are selected based upon the maximum allowable values for both the CEM and the photoresist.

3.4.1 Energy Increments for Resist

The determination of the energy increments required for the underlying photoresist has not been changed from SAMPLE version 1.6a.[12] The energy increments are selected such that an unexposed layer on a matched substrate will change its M value by ΔM for a given energy increment, ΔE. Assuming that the M values change by about 0.7 over the entire exposure, then ΔM is given by:

$$\Delta M = \frac{0.7}{N_E}$$

where N_E is the number of energy increments. The absorption in the photoresist is assumed to be small enough that M is constant throughout the entire thickness of photoresist for this approximation. This results in:

$$\Delta E = \frac{\ln(1 - \Delta M)}{C e^{-(A + B)\, d}} \tag{3.6}$$

where d is the total photoresist thickness.

3.4.2 Energy Increments for CEM

Since the absorption in the CEM is much higher than photoresist, it can no longer be assumed that the M value is approximately constant over the entire thickness. It can be assumed, however, that the M values is constant over the thickness of each of the layers that the CEM is subdivided into for the bleaching algorithm. As shown in Figure 2, each layer of the CEM can be described by an energy increment at the top ΔE_{i-1} ($\Delta E_0 = \Delta E$, the actual energy increment at the surface), the amount that leaves the bottom ΔE_i, an M value, M_i, and a thickness d_i. The ratio of ΔE_i to ΔE_{i-1}, g_i, describes the amount of energy absorbed in the i^{th} layer. This is given by:

$$g_i = \frac{\Delta E_i}{\Delta E_{i-1}} = e^{-(AM_i + B)\, d_i} \tag{3.7}$$

Or, the ratio of ΔE_i to ΔE, defined as f_i, can be described by:

$$f_i = \frac{\Delta E_i}{\Delta E} = f_{i-1}\, e^{-(AM_i + B)\, d_i} \tag{3.8}$$

where $f_0 = 1$. Using equation 3.4 and assuming no reflections:

$$M_i - \Delta M_i = M_i \, e^{-C \, \Delta E_{i-1}} \tag{3.9}$$

Substituting for ΔE_{i-1} with equation 3.8 and solving for ΔE results in:

$$\Delta E = \frac{\ln(M_i) - \ln(M_i - \Delta M)}{f_{i-1} \, C} \tag{3.10}$$

for a given ΔM which has the same value as that described in Section 3.4.1. ΔE is calculated for each of the layers within the CEM and the minimum value selected as the energy increment required for the CEM. This procedure is carried out for each energy increment.

When these equations are implemented, the energy increments start to increase too fast when the M values in the CEM approach zero. This is corrected by averaging the calculated energy increment with the first increment (the smallest one since all M_i's are 1) so that the size of the increase is halved.

3.4.3 The Combined Increment

The combined increment is selected by examining the energy increments needed by both the CEM and the photoresist. Qualitatively, at the beginning of the exposure, the CEM is very opaque, and the photoresist receives very little energy. At this point, therefore, the selection of the energy increments is dominated by the energy increment required by the CEM. Near the end of exposure, however, the CEM is almost completely transparent, and the photoresist is receiving almost all of the energy. If the photoresist is sufficiently sensitive, then the energy increments will, at this point, be dominated by the energy increment required by the photoresist. Somewhere in the middle, the increments must be switched from one case to the other.

The above description is implemented as follows. If the portion of the CEM energy increment that passes completely through the CEM is less than the maximum size required for the photoresist, then the CEM energy increment is used. But, if that amount is greater than the photoresist energy increment, then the routine switches over to the photoresist energy increments. The number of subdivided layers in the CEM can be defined by L. Then, the term f_L from equation 3.8 is the the amount of the energy increment leaving the CEM divided by the size of the energy increment at the CEM surface. The condition for using the CEM energy increment is:

$$\Delta E_{cem} f_L < \Delta E_{res} \tag{3.11}$$

The condition for using the photoresist energy increment is:

$$\Delta E_{res} < \Delta E_{cem} f_L \tag{3.12}$$

In the SAMPLE routine for one layer of photoresist, to increase speed and reduce the amount of stored values, the calculated photoresist energy increment is compared with 15 percent of the total dose and the maximum value used. A similar method is used in the CEM routine, except for the photoresist energy increment is compared with 15 percent of the total dose minus the dose where the energy increments are switched over to the photoresist increments.

3.4.4 Variable Storage of M Values

When a single layer of photoresist is used in SAMPLE, the number of energy increments needed for typical doses is usually less than 15. However, when CEM is used, a large number of energy increments is often required. Previously, for each energy increment, the M values for each subdivided layer was stored in a matrix. If this approach was taken for CEM, the matrix would become too large. To alleviate this problem, the CEM routine has been implemented so that instead of storing the M values for every increment, they are stored every N_s increments, where N_s depends on the CEM parameters and the degree of exposure. With possible usage on the IBM PC in mind, it was decided that the total number of stored energy increments should be less than 30. Also, no matter what the parameters of the CEM are, the number of stored increments should be relatively constant.

The energy that is required to bleach a layer of CEM of thickness d is proportional to $\frac{Ad}{C}$. But, according to equation 3.10, the energy increment required by the CEM is also inversely proportional to C. Therefore, even as C changes, the number of energy increments required to bleach the CEM should stay relatively constant. Equation 3.10 has no dependence on A and d, though, so N_s is chosen to be proportional to Ad. Once the dose has gone beyond the point where the energy increments for the photoresist are being used, every energy increment is stored as before.

3.5 New Method Using Analytical Solution to Dill's Equations

3.5.1 The Babu and Barouch Solution

During the initial stages of exposure, the CEM is still quite opaque, and most of the energy is absorbed before reaching the underlying resist. Therefore, an assumption of a nonreflecting substrate beneath the CEM would be a good approximation of the actual situation. Babu and Barouch[8] have proposed an analytical solution to Dill's equation, 3.1 and 3.2, for nonreflecting substrates. The solution is:

$$\int_{M_0}^{M(z)} \frac{dx}{x\,[A\,(1-x) - B\,\ln x]} = z \tag{3.13}$$

where z is the depth into the photoresist (or CEM) and M_0 is the M value at the surface. The simulation of the exposure of CEM can now be performed by an initial analytical solution given by Babu and Barouch, and then by the numerical solution described in section 3.3 when the approximation of a nonreflecting substrate beneath the CEM breaks down. The use of this solution reduces both computation time and the number of stored M values since several initial energy increments can be replaced by the analytical solution.

3.5.2 Implementation

To implement the solution by Babu and Barouch, the point where the approximation is no longer valid is required. After comparing the M values in the CEM from both the analytical and numerical solutions, M = 0.95 at the CEM/photoresist interface was chosen as the switch point. To determine the dose that corresponds to this point, equation 3.13 is integrated numerically using a Gaussian quadrature routine. First, z is set equal to the thickness of the the CEM and M(z) set equal to 0.95. Then, M_0 is systematically reduced, starting from 0.95, and the integration performed until the equality is met and M_0 is obtained. From Dill's equations with a nonreflecting substrate:

$$M_0 = e^{-CD_i} \tag{3.14}$$

where D_i is the dose required to have M_0 at the surface, and, therefore, M = 0.95 at the interface. Note that this dose corresponds to the dose right inside the surface of the CEM, or, in other words, after front surface reflection. Next, the M values between the surface and the interface are determined. Since M_0

is now known, for a given z in equation 3.13, M(z) is increased, starting from M_0, and again the integration is performed until the equality is met and and M(z) obtained. This is repeated for every value of z, so that after completion, the M values are known throughout the CEM.

Since the index of refraction changes (real and imaginary parts) as the M at the surface changes, the front surface reflection is not constant over the duration of the analytical solution. The front surface reflection term is approximated by calculating an average M value at the surface. It can be shown that given D_i, the dose without front surface reflection, the average M value is:

$$M_{ave} = \frac{1 - e^{-CD_i}}{CD_i} \tag{3.15}$$

An average index of refraction and thus an average front surface reflection coefficient, r_{ave}, can now be calculated. Then:

$$D_e = \frac{D_i}{1 - r_{ave}^2} \tag{3.16}$$

where D_e is the external dose, including front surface reflection, to get M = 0.95 at the interface. D_e corresponds to the first energy increment for the numerical solution and the calculated M values are the first entries in the storage matrix. The larger D_e is compared to the first energy increment required for the numerical solution, the larger the benefit in using the Babu and Barouch solution.

As D_i gets larger, M_0 gets smaller. But, in equation 3.13, the integrand approaches infinity as x approaches 0. Numerical integration becomes very difficult in this region since the size of the integration steps must be made very small for an accurate solution. To solve this problem, equation 3.13 is written as:

$$\int_{M_1}^{M(z)} \frac{dx}{x\,[A\,(1-x) - B \ln x]} + \int_{M_0}^{M_1} \frac{dx}{x\,[A\,(1-x) - B \ln x]} = z \tag{3.17}$$

where $M_1 \ll 1$ and in this case is chosen to be 10^{-4}. The first integral is solved numerically as before. The second integral, with the given condition on M_1, is approximated to get an analytical solution. Assuming that T is the solution to the numerically integrated term and d is the thickness of the CEM, then it can be shown that:

$$D_i = \frac{(A - B \ln M_1)\, e^{B(d-T)} - A}{BC} \tag{3.18}$$

M can also be solved for at every depth in the CEM, z, up to the depth where $M = M_1$ resulting in:

$$M = \exp\left[\frac{A - (BCD_i + A)\, e^{-Bz}}{B}\right] \tag{3.19}$$

3.5.3 Modifications for Underlying Resist

If the solution by Babu and Barouch was completely valid in the described case, then all of the energy incident on the CEM would be absorbed before reaching the underlying photoresist. This is not strictly true, however, since M = 0.95 in the CEM at the interface. Therefore, a small correction dose is applied to the photoresist beneath. Since M = 0.95 at the interface, from Dill's equations, the extra dose given to the photoresist, D_r, is given by:

$$D_r = \frac{-\ln 0.95}{C} \tag{3.20}$$

where C is the value for the CEM. The Berning algorithm is modified for this correction dose given to the photoresist only. The ambient index of refraction, though must be changed to that of the CEM instead of air. The Berning algorithm only uses an ambient index of refraction that is real, however, so the index of refraction of the CEM is modified for this algorithm so that it is purely real. This is done by computing an effective index of refraction that results in the same reflectivity at the interface that occurs with the actual refractive index. Shown in Figure 3 are M values for both the numerical solution and the Babu solution for a simple test case. Figure 4 shows how well the final photoresist profiles match for the same test case.

3.5.4 Limitations and Problems

Several limitations exist when using the Babu and Barouch solution in the simulation of contrast enhanced lithography. As of this report, no modification to the solution for multiple wavelengths has been derived. The complete numerical solution must be used when several wavelengths are present. Also, no approximation is made concerning the energy that is reflected at the CEM/photoresist interface or that is reflected at the photoresist/substrate interface and passes back through the CEM. This approximation can have serious drawbacks when the substrate is highly reflective as in aluminum.

Whenever, there is significant internal reflection in the CEM, the solution becomes inaccurate.

This occurs, for example, when A is very large. This is because the extinction coefficient, which is proportional to AM as seen in equation 3.1, may vary dramatically between regions of low and high M. These regions can become very close to each other as A is increased because the absorption is extremely high. Figure 5 shows the M values for a layer of CEM with $A = 30\ \mu m^{-1}$ using both the Babu solution and SAMPLE with one layer of CEM on a matched substrate. Since SAMPLE includes all of the internal reflections, it can be seen from Figure 5 that some of the incident energy is reflecting off of the region with high M values back into the region with lower M values. Therefore, the front of the layer is exposing even faster than predicted by Babu's solution, and the back of the layer is bleaching slower than expected. Figure 6 shows how the difference between the two curves gets worse as the extinction coefficient is increased by using a longer wavelength (see equation 3.1). It is believed, however, that the parameters that cause the above problems are well outside the range of standard usage. The same type of problems could be expected when the bleachable model for the real part of the index of refraction is used, but so far no inaccuracies have been observed.

According to Babu and Barouch,[13] a new solution will be available that takes all reflections into account. An implementation of this solution may alleviate many of the problems discussed above.

Chapter 4

Applications and Examples

4.1 Introduction

A method has been proposed in Chapter 3 for simulating contrast enhanced lithography. In this chapter, the modified SAMPLE program (version 1.7a) is used to explore the advantages and limitations of using CEM. CEM is compared with a standard photoresist process, as well as other promising techniques such as anti-reflection coatings and bilayer resist processes.

4.2 Comparison With Standard Resist Process

4.2.1 Profile Quality

The resolution capabilities of a CEM process can be compared to that of a standard photoresist process with the modified SAMPLE program. For both processes, the simulation parameters correspond to a stepper with a wavelength of $\lambda = 436$ nm, a numerical aperture of NA = .28 and a partial coherence factor of $\sigma = 0.7$. Shown in Table 4.1 are the parameters used for the CEM and the photoresist.

Table 4.1 -- Photoresist and CEM Simulation Parameters

Material	A (μm^{-1})	B (μm^{-1})	C (cm^2/mJ)	thickness (μm)	E1	E2	E3
Resist	0.551	0.058	0.010	0.713	5.63	7.43	-12.6
CEM	12.00	0.001	0.064	0.400	----	----	-----

The minimum resolution of a standard photoresist process on silicon is generally considered to be 0.8λ/NA. With the parameters given above, this corresponds to a feature size of about 1.25 μm. The furthest curve on the right in Figure 7 is the simulated photoresist profile without CEM for a 1.25 μm line and space pattern. The curve on the left in Figure 7 also simulates a photoresist profile without CEM, but for a 0.75 μm line and space pattern. This feature size corresponds to about 0.5λ/NA. As

can be seen from the profile, for the same dose and development time, the photoresist is no longer able to effectively print the smaller feature. The photoresist does not develop through to the substrate, and the slope of the profile has deteriorated. Also shown in Figure 7 is the photoresist profile when CEM is used for the same 0.75 μm image. There is a dramatic improvement in the quality of the profile over the profile with photoresist alone. In fact, the slope of the profile appears to be as vertical as the profile for the 1.25 μm pattern with photoresist only, with the added benefit of a reduced standing wave effect. Apparently this reduction is due to the CEM sharpening the image seen by the photoresist such that horizontal development has been retarded. Therefore, while the developer is trying to break through a null point in the standing wave pattern, it is less likely to etch sideways in the peak exposure areas. The improvement in the profile comes at the expense of exposure time, however. The dose for the CEM process is 2.4 times greater than the dose for the standard photoresist process.

4.2.2 Exposure Latitude

The exposure latitude of each process can also be compared by simulation. The same photoresist and CEM parameters from Table 4.1 are used again. Both the single layer photoresist and the CEM/photoresist system in this case are exposed with a 1.0 μm equal line and space pattern. The nominal dose is selected so that the linewidth at the base of the photoresist is equal to the mask linewidth. The nominal profiles for each case are shown in Figures 8 and 9 (solid lines). The photoresist systems in both cases are then subjected to a 15 percent overexposure and a 15 percent underexposure. As seen in Figures 8 and 9, the linewidth measured at the base of the photoresist changes much less when the CEM is used. The single layer photoresist does not develop through to the substrate when underexposed, while the CEM process still results in a usable photoresist profile.

Figure 10 shows the change in linewidth versus percent change in exposure for a standard photoresist and a CEM process. In this simulation, the photoresist thickness is 1.5 μm and the other parameters are the same as in Table 4.1. The mask is a 1.2 μm line and space pattern. Figure 11[4] shows experimental results obtained by West et al. for the same mask pattern. Several parameters are either not the same as the parameters used in the simulation or are not known. Therefore, these results are presented only to show that the basic trends of the simulation are similar to the trends seen

experimentally.

Often, real photoresist processes are overexposed to gain linewidth control at the expense of a bias between the mask and the actual photoresist profile. This gain is seen clearly from the reduced slope of the photoresist curve of Figure 10 in the overexposed region. The improvement in linewidth control with CEM would not be as much as seen in Figures 8 and 9 in this region of operation. If the thickness of the CEM changed significantly, the linewidth variation could conceivably be worse for CEM than the biased photoresist process since the energy reaching the underlying photoresist would change as the CEM thickness changed.

4.3 Comparison with Anti-Reflection Coatings

An anti-reflection coating (ARC) is a layer that coats the substrate to reduce the standing wave ratio in the photoresist. This reduction in the substrate reflectivity allows the printing of smaller features and results in better linewidth control. ARC's can be simulated in SAMPLE by changing the index of refraction of the substrate until the desired reflectivity is obtained, or by including a stack of thin films that is used in the real ARC process.

4.3.1 ARC with Silicon Substrate

Figure 12 is a comparison between a standard photoresist process, an ARC used with the same standard photoresist process, and a CEM process. A silicon substrate is used for the simulation. Again, all the photoresist and CEM parameters are given in Table 4.1. The mask is a 0.75 μm, or 0.5λ/NA, equal line and space pattern. The profile furthest to the left results from the standard photoresist process. The slope of the profile is slanted, and much of the top has been developed away. The profile in the middle with the standing wave pattern corresponds to the use of an ARC that reduces the reflection coefficient by a factor of 2. Obviously, the ARC has improved the slope of the profile as well as reduced the standing wave pattern. The smooth curve in the middle is for a completely matched substrate. This profile demonstrates the largest possible improvement from using an ARC. Even with all reflections removed, the contrast of the image is still poor enough to limit the slope of the photoresist profile. The final profile on the right is obtained with the CEM process. The CEM profile

has the most vertical slope of all of the cases. It is also interesting to see that the CEM has reduced the standing wave ratio as much as the ARC with the reduced reflection coefficient did. This is again due to the CEM improving the image seen by the photoresist which reduces the horizontal development as described in section 4.2.1. From Figure 12, therefore, it can be concluded that when the process is limited by the contrast of the aerial image, CEM will offer a larger improvement to the photoresist profile than an ARC.

4.3.2 ARC with Aluminum Substrate

Patterning on aluminum is much more difficult than on silicon because of the higher reflectivity of aluminum. The minimum feature size on aluminum is usually quoted as $1.1\lambda/NA$ as opposed to $0.8\lambda/NA$ on silicon. The linewidth is also difficult to control due to the large difference in development rates between the peaks and the nulls of the standing wave pattern.

Figure 13 shows photoresist profiles on aluminum when ARC, CEM, and a combination of ARC and CEM are used. The mask pattern is a 1.0 μm line and space pattern which is equivalent to $0.65\lambda/NA$. The ARC is simulated by a 50 percent reduction in the reflection coefficient of the substrate. Both the CEM and the ARC processes produce photoresist profiles with almost vertical slopes. The ARC, however, has reduced the standing wave ratio much more than the CEM has. An excellent profile results from using both CEM and ARC, but this also requires the most complex process. According to the simulations, therefore, CEM will improve the slope of photoresist profiles on aluminum, but large standing waves in the photoresist are still a problem. ARC can improve the profile, while at the same time significantly reducing the reflectivity problems. More problems with CEM on aluminum will be discussed in section 4.4.5.2.

4.4 Comparison with Bilayer Resist Process

4.4.1 Introduction

Another method to improve the resolution capability of the resist system is the bilayer resist, or portable conformable mask (PCM)[14] process. Recently, a joint study was done with E. Ong and B. Singh[15] of Advanced Micro Devices (AMD) to examine the performance of both the CEM and the

PCM processes in terms of linewidth control and proximity effects as a function of feature size, dose, focus, and substrate reflectivity. Proximity effects are defined as any changes in feature size caused by other features in close proximity. For example, proximity effects exist if an equal line and space pattern and an isolated line of the same size on the mask are not the same size on the wafer.

4.4.2 PCM Process Description

The highest resolution for a single layer of photoresist is obtained when the photoresist is thin. In a single layer photoresist process, however, large variations in substrate topography dictate that a thicker photoresist be used. Also, as pointed out earlier, higher resolution is obtained when there are no reflections from the substrate. In the PCM process, a thick, dyed layer is deposited to planarize the substrate and reduce reflections from the substrate. Then, a thin photoresist layer is spun on top which can then be imaged at the highest possible resolution. The top layer then acts as a mask as the pattern is transferred by either exposure and development or plasma etching of the bottom layer.

4.4.3 Experimental Work

Experiments were done at AMD by Ong and Singh[15] to compare the resolution of the two processes. In the CEM process, a 0.6 μm layer of CEM-420 was used on top of 1.8 μm of AZ 1350J photoresist. In the PCM process, the bottom layer was a 1.6 μm layer of dyed PMMA, while the top layer was 0.8 μm of AZ 1350J photoresist. The substrates consisted of wafers coated with either 0.3 μm of polysilicon or 1.0 μm of aluminum. The wafers were patterned with a Prometrix mask with different feature sizes and types using a GCA 5:1 stepper with $\lambda = 436$ nm, NA = 0.30, and $\sigma = 0.5$. The substrates were then etched after the photoresist was exposed and developed. Linewidths were measured using the Prometrix electrical linewidth tester.

4.4.4 Simulations

Both the CEM and PCM processes were also examined using the modified SAMPLE program and the results compared with the experimental data.[15] It was assumed that in the PCM process, the transfer of the pattern in the top layer by the deep UV exposure of the underlying PMMA had no effect on the linewidth. Therefore, the PCM process was modeled by a single layer of thin photoresist on top of a

matched substrate since the underlying PMMA layer contained a heavily absorbing dye. The exposure parameters used for the photoresist are the same as those given in Table 4.1. The dissolution parameters (R parameters) are given in Table 4.2.

The parameters used to describe the CEM are given as the third entry of Table 3.1. The exposure parameters for the photoresist are the same as for the PCM. However, as can be seen by the SEM of Figure 14, the CEM can cause an induction effect at the surface of the underlying photoresist. An attempt was made to model this development effect by changing the R parameters of the photoresist to match the simulated profile (see for example Figure 17) to the profile in the SEM. Future work is needed to better model this effect. The altered R parameters used for the CEM effected photoresist are given in Table 4.2.

Table 4.2 -- R Parameters for Photoresist in CEM and PCM Processes

Process	R1 (μm/sec)	R2 (μm/sec)	R3	R4 (μm)	R5	R6
PCM	0.24	0.0005	8.1	0.24	0.76	0.55
CEM	0.24	0.0005	8.1	0.30	0.0005	5.e-11

4.4.5 Results

4.4.5.1 Silicon Substrate

Figure 15 shows the experimental results for the CEM and PCM processes on the polysilicon substrates. Compared on each graph are the differences in linewidth from the mask for equal line and space and isolated line patterns. Values are given at two doses for several different feature sizes. Using PCM, the isolated line is slightly larger than the line and space pattern over the entire range of feature sizes. The CEM isolated lines are slightly larger than the line and space pattern for the larger feature sizes, but become slightly smaller at the smaller feature sizes. In both processes, the change in linewidth due to changes in exposure is always less than 0.2 μm.

Figures 16 - 18 show the simulation results of 1.0 μm features on a silicon substrate covered by a one half wavelength thick oxide layer. In Figure 16, the isolated line is slightly larger than the equal line and space pattern with the PCM process, as in the experimental results. In Figure 17 as well, almost no proximity effect is seen with the CEM process as was shown experimentally. The isolated line in this case, though, is slightly larger than the equal line and space pattern in the simulation, but slightly smaller in the experiments. Figures 16 and 17 also show that the linewidths for both CEM and PCM are not strongly affected by 3.0 μm. Just as the linewidths changed only slightly from overexposure experimentally, the simulations of Figure 18 show that even with 40 percent overexposure, the linewidths for both processes change by less than 20 percent.

4.4.5.2 Aluminum Substrate

Figure 19 shows the experimental results for the aluminum substrates. The results for the PCM process are similar to those from the polysilicon substrates. Again, the isolated line is only slightly larger than the equal line and space pattern, and overexposure reduces the linewidths by less than 0.2 μm. These results are to be expected since the dyed PMMA layer absorbs most of the energy before it reaches the substrate.

In the experimental results for the CEM, it is clear that the performance of the CEM process has deteriorated with respect to the PCM process. The isolated line is now much smaller than equal line and space pattern, and overexposure has resulted in a significant reduction in linewidth. In the simulations of Figure 20, though, the isolated line is still slightly larger than the line and space pattern, and the linewidth change due to overexposure is not significantly different than the change seen on the silicon substrates. These discrepancies indicate that additional mechanisms are present when the substrate reflectivity becomes dominant.

Several possibilities may explain the poorer performance of CEM on aluminum that was demonstrated experimentally, but not seen in simulations. One possibility is the forward scattering of light by large particles in the CEM resulting in a lower quality image at the CEM/photoresist interface. As the substrate reflectivity is increased, this effect would intensify since light that is reflected at the substrate travels approximately twice the horizontal distance in the photoresist as the light that is not reflected.

An experiment was done with W. Haller to examine the forward scattering in CEM compared to photoresist. A laser at 633 nm was focused on glass substrates coated with CEM-420 and Kodak 820 photoresist. The transmitted light was recorded as a function of angle. Figure 21 shows that thin layers of both CEM-420 and Kodak 820 photoresist do not significantly scatter light in comparison to air. Therefore, forward scattering in the CEM is apparently not the problem.

Lateral scattering from the substrate into the masked areas could also account for the feature type dependent effects seen on aluminum substrates. The roughness of the substrate of Figure 22 confirms that this is a definite possibility. The notching in the photoresist, as well, could be due to the incident energy not being reflected uniformly from the substrate. Flare would also be much more prevalent around isolated features surrounded by a highly reflecting substrate. SAMPLE simulations show, however, that an increase in flare of at least six percent is required to cause the images of the two feature types to cross over at the operating point.

If the linewidths in the CEM process were determined by a given threshold in the incident image, such as the 30% point, then the isolated line would be larger than the line and space pattern as is seen in the simulations. However, the peak intensity of the clear area in the line and space pattern is smaller than the intensity at the same position in the clear area for the isolated line. This difference in the intensity might result in the developer breaking through to the substrate first in the isolated line pattern. It would be possible, then, for the developer to be etching horizontally on the isolated line for a longer time resulting in a smaller final profile. This effect would increase for smaller features, just as seen experimentally, since the peak intensity in the clear area of the line and space pattern decreases for smaller feature sizes. This pattern dependent difference in dissolution delay is dependent upon photoresist thickness, exposure level, and photoresist dissolution parameters. If the photoresist dissolution parameters were selected such that the development rates were not as different for these two peak intensities as they were experimentally or, if too much overdevelopment was used in the simulation, then this horizontal development effect in the isolated line case would be reduced. Further simulations with different development parameters are needed to examine this issue.

Chapter 5

Conclusion

Modifications to SAMPLE have been implemented in version 1.7a for the simulation of contrast enhanced lithography. Exposure coupling effects between the CEM and the underlying photoresist have been included by the simultaneous bleaching of both materials. This rigorous approach also includes the capability of simulating exposures on arbitrary stacks of thin film substrates that produce standing waves in both the photoresist and CEM. The exposure model for the CEM is based on Dill's model for the exposure of positive photoresist. Also included in the model is a refractive index that changes as the CEM is exposed. Since the CEM is both highly absorptive and has significantly different bleaching properties than the underlying photoresist, selection of the energy increments for the numerical exposure algorithm becomes quite difficult. A method has been described that calculates the energy increments based upon the energy increments required for both materials. Initially, most of the energy is absorbed in the CEM, and therefore, the CEM energy increment is used. When the CEM becomes almost completely transparent, the photoresist energy increment is used. An analytical solution for the initial stages of exposure in the CEM that uses Babu and Barouch's solution for matched substrates has also been implemented. The new routine switches from the analytical to the numerical solution when a significant amount of energy passes through the CEM to the photoresist which invalidates the approximation of a matched substrate beneath the CEM. Several steps in the numerical solution are eliminated with this method resulting in faster speeds and less storage.

The modified SAMPLE program has been used to explore some of the capabilities of contrast enhanced lithography. The resolution of CEM is superior to a standard photoresist process in simulation. CEM also has better linewidth control than a photoresist process with no bias. Linewidth control with CEM is also better than a standard photoresist process with bias if changes in the CEM thickness are minimal. The CEM process has been compared to other techniques for improved resolution as well. According to simulation, the resolution of CEM on silicon is better than the resolution of an ARC process. On highly reflecting substrates such as aluminum, however, the ARC process reduces the standing wave pattern more than the CEM process. Bilayer resist (PCM) and CEM processes are equivalent in

resolution, linewidth control and proximity effects in both simulation and experiments on silicon substrates. Simulation shows that on aluminum the performances of both processes are similar. Experimentally, however, the CEM suffers from reflective notching and a large proximity effect as the isolated line becomes much smaller than the line and space pattern. Possible explanations include lateral scattering from the substrate, flare, and a difference in dissolution delay in nearby clear areas caused by the pattern dependent intensity maximums there.

The SAMPLE program is now capable of providing a fundamental understanding of some of the key issues in contrast enhanced lithography. Accuracy of the analytical solution by Babu and Barouch can be explored in cases where the real or imaginary parts of the refractive index change. The CEM exposure model incorporated in SAMPLE can be used to examine the effects of a changing index of refraction on the performance of the CEM. The program is also useful in designing experiments to measure the parameters to be used in the bleachable refractive index model. The effects of standing waves in the CEM on the contrast gain can be studied by using substrates with different reflectivities. To optimize the CEM process, the best bleach rate for the CEM for a given bleach rate of the underlying photoresist can be determined through simulations with different C parameters. The importance of the dissolution parameters of the underlying photoresist in determining the size of proximity effects can be analyzed. Also, tradeoffs between the performance of the CEM and the increase in the dose required for exposure can be studied.

References

1. W. G. Oldham, S. N. Nandgaonkar, A. R. Neureuther, and M. M. O'Toole, "A General Simulator for VLSI Lithography and Etching Processes: Part I - Applications to Projection Lithography," *IEEE Trans. Electron Devices*, vol. ED-26, no. 4, pp. 717-722, April 1979.

2. B. F. Griffing and P. R. West, "Contrast Enhanced Photolithography," *IEEE Electron Device Lett.*, vol. EDL-4, no. 1, pp. 14-16, Jan. 1983.

3. P. R. West and B. F. Griffing, "Contrast Enhancement - A Route to Submicron Optical Lithography," *Proceedings of SPIE*, vol. 394, pp. 33-38, March 16-17.

4. P. R. West, J. C. Sardella, and R. E. Williams, "Chemistry and Processing in the Design and Evaluation of a G-line Contrast Enhancement Material," *Proceedings of SPIE*.

5. M. M. O'Toole, "Simulated Performance of a Contrast Enhancement Material," *IEEE Electron Device Lett.*, vol. EDL-6, no. 6, pp. 282-284, June 1985.

6. A. R. Neureuther, D. C. Hofer, and C. G. Willson, "Design of Contrast Enhancement Processes for Optical Lithography," *Microcircuit Engineering*, pp. 53-60, Academic Press, 1985.

7. W. G. Oldham, "The Use of Contrast Enhancement Layers to Improve the Effective Contrast of Positive Photoresist," *IEEE Trans. Electron Devices*, vol. ED-34, no. 2, pp. 247-251, February 1987.

8. S. V. Babu and E. Barouch, "Exact Solution of Dill's Model Equations for Positive Photoresist Kinetics," *IEEE Electron Device Lett.*, vol. EDL-7, no. 4, pp. 252-253, April 1986.

9. F. H. Dill, W. P. Hornberger, P. S. Hauge, and J. M. Shaw, "Characterization of Positive Photoresist," *IEEE Trans. Electron Devices*, vol. ED-22, no. 7, pp. 445-452, July 1975.

10. B. F. Griffing and P. R. West, "Contrast Enhanced Photoresists - Processing and Modeling," *Polymer Engineering and Science*, vol. 23, no. 17, pp. 947-952, Mid-December 1983.

11. P. H. Berning, "Theory and Calculations of Optical Thin Films," in *Physics of Thin Films*, vol. 1, pp. 69-120, 1963.

12. M. M. O'Toole, "Simulation of Optically Formed Image Profiles in Positive Photoresist," PhD Thesis, Dept. of EECS, U.C. Berkeley, June 1979.

13. S. V. Babu and E. Barouch. Private communication, March 1987

14. B. J. Lin, E. Bassous, V. Chao, and K. Petrillo, "Practicing the Novolac Deep-UV Portable Conformable Masking Technique," *J. Vac. Sci. Technol.*, vol. 19, p. 1313, 1981.

15. E. Ong, B. Singh, R. Ferguson, and A. Neureuther, "Comparison of Proximity Effects in Contrast Enhancement Layer and Bilayer Resist Processes," *Proc. 30th Int. Symposium on Electron, Ion, and Photon Beams*, pp. 443-448, May 27-30, 1986.

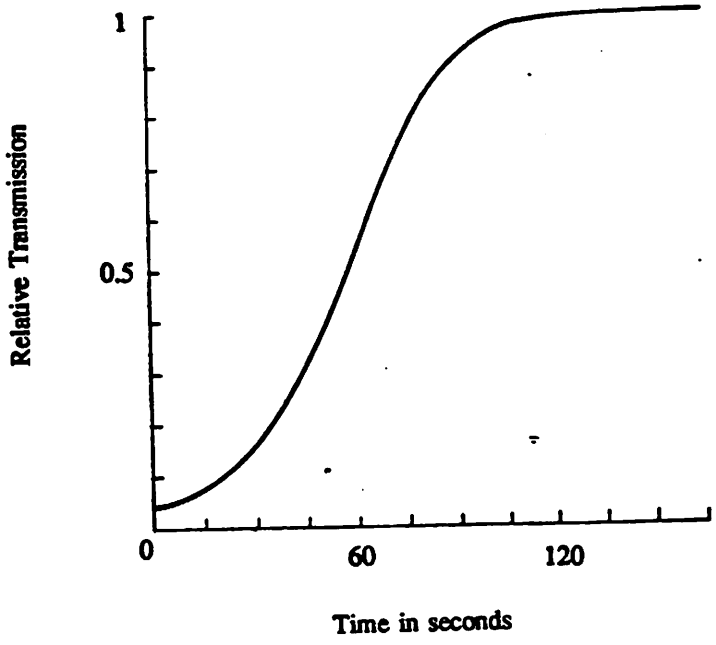

Figure 1. Transmission versus time for a .25 μm layer of CEM-388. Exposure intensity is 0.67 mw/cm^2 with $\lambda = 405$ nm.

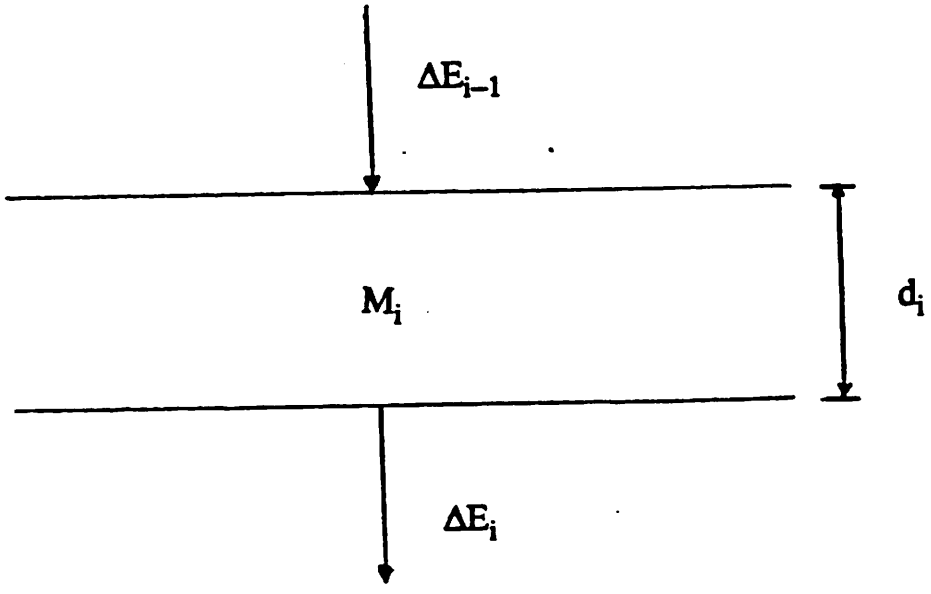

Figure 2. Configuration of i_{th} layer of CEM for calculating energy increments.

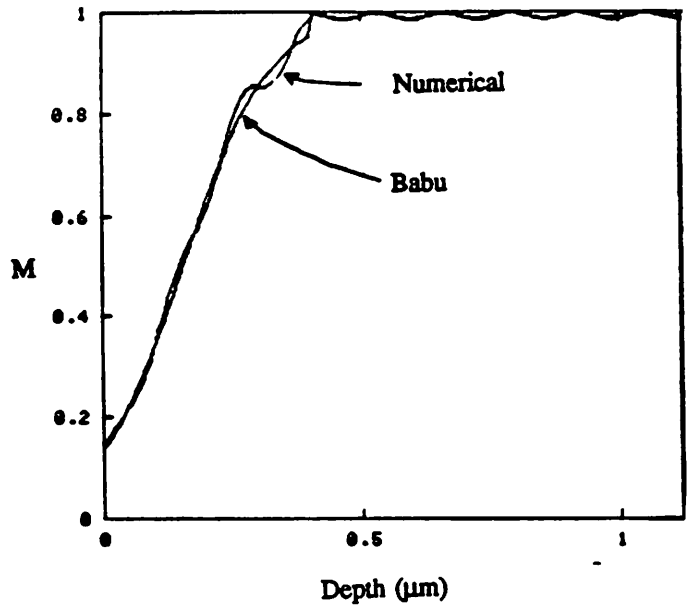

Figure 3. M values versus depth for Babu and Barouch solution and numerical solution. CEM is 0.4 μm thick and resist is 0.71 μm thick. Other parameters given in Table 4.1.

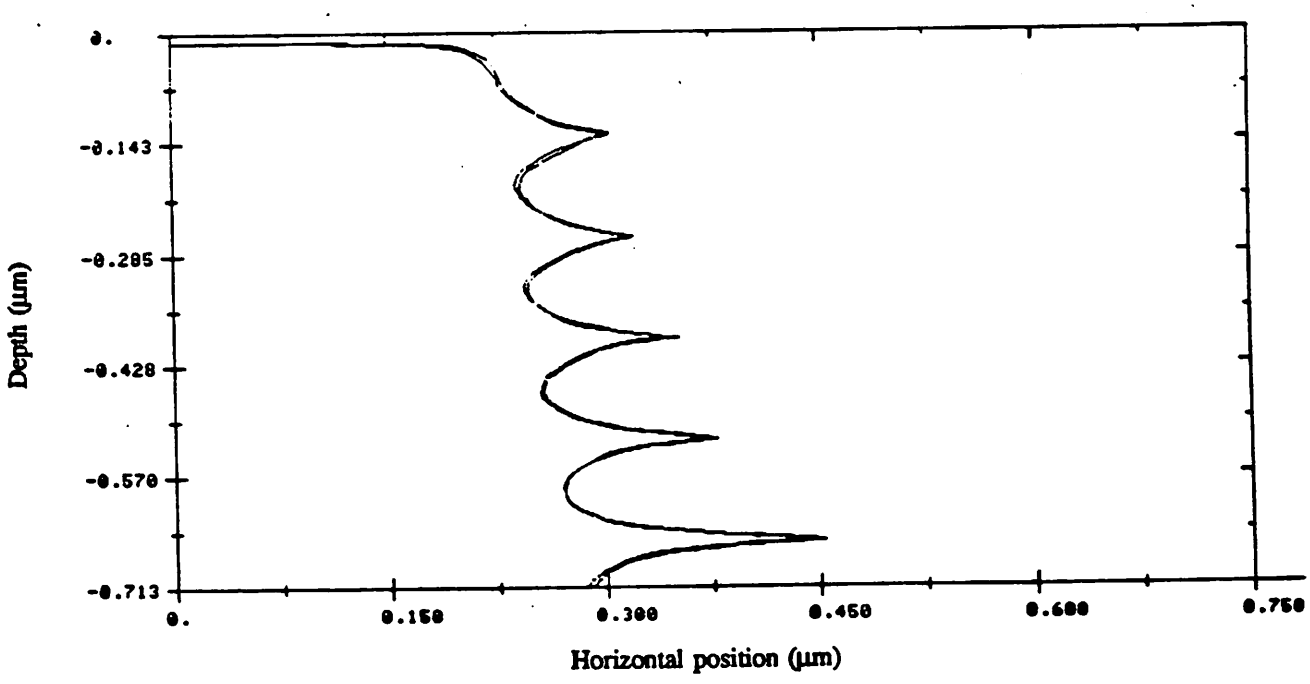

Figure 4. Photoresist development profiles for Babu and Barouch solution and numerical solution from test case described in Figure 3. Mask pattern is 0.75 μm equal line and space pattern.

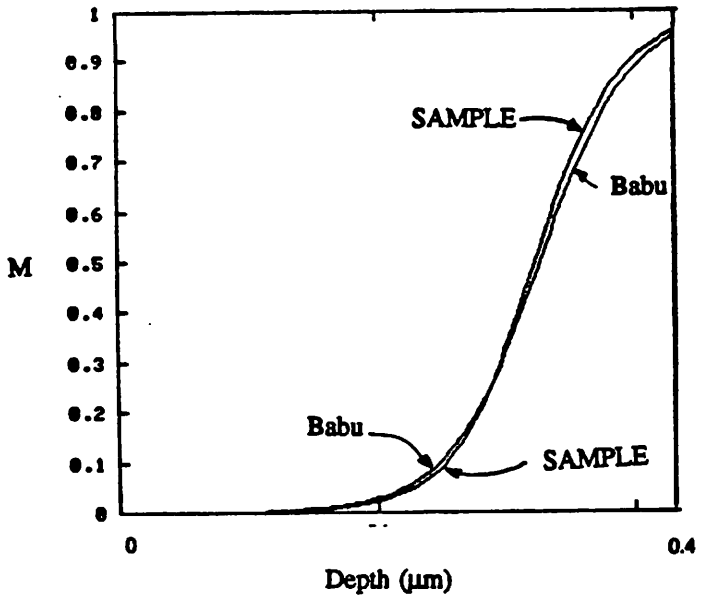

Figure 5. M values versus depth for Babu and Barouch solution and SAMPLE with layer of CEM on a matched substrate. CEM is 0.4 μm thick. $A = 30\ \mu m^{-1}$, $\lambda = 436$ nm.

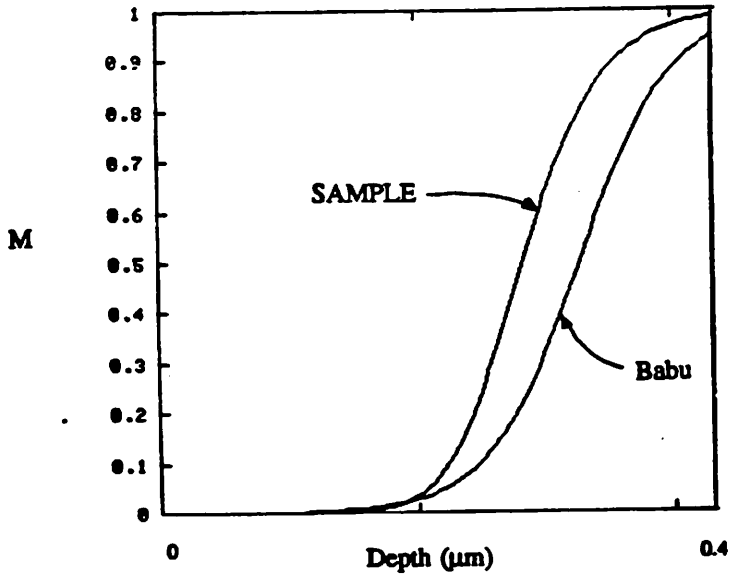

Figure 6. M values versus depth for Babu and Barouch solution and SAMPLE with layer of CEM on a matched substrate. CEM is 0.4 μm thick. $A = 30\ \mu m^{-1}$, $\lambda = 1000$ nm.

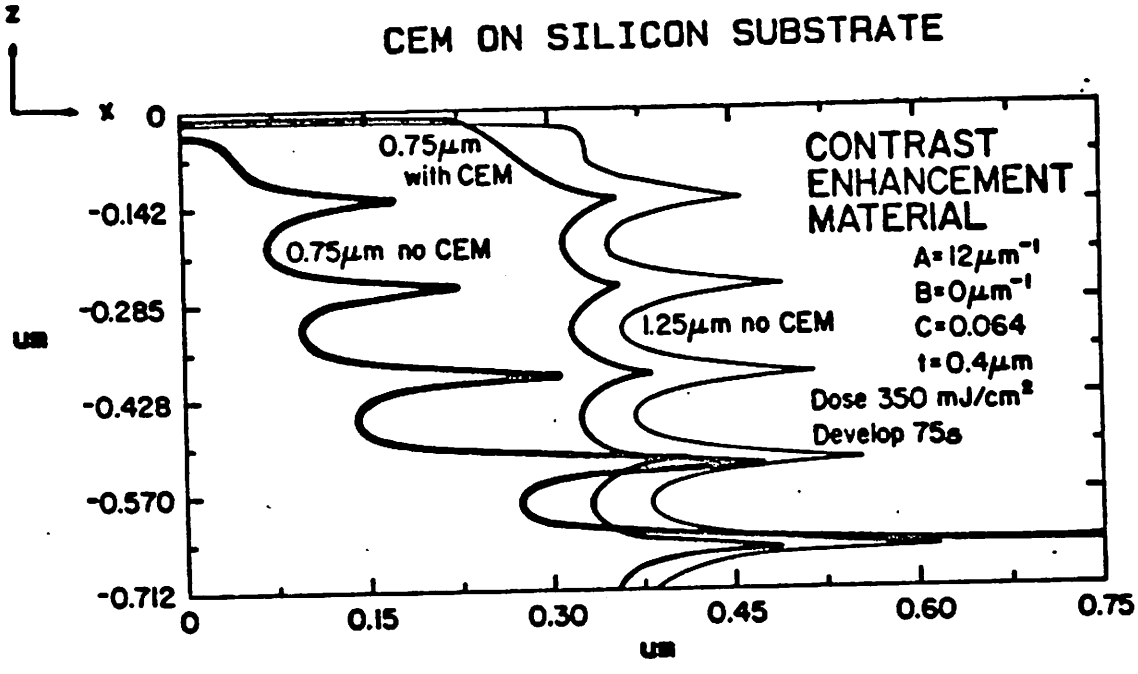

Figure 7. Photoresist development profiles for 1.25 μm (0.8λ/NA) and 0.75 μm (0.5λ/NA) patterns without CEM and 0.75 μm (0.5λ/NA) with CEM.

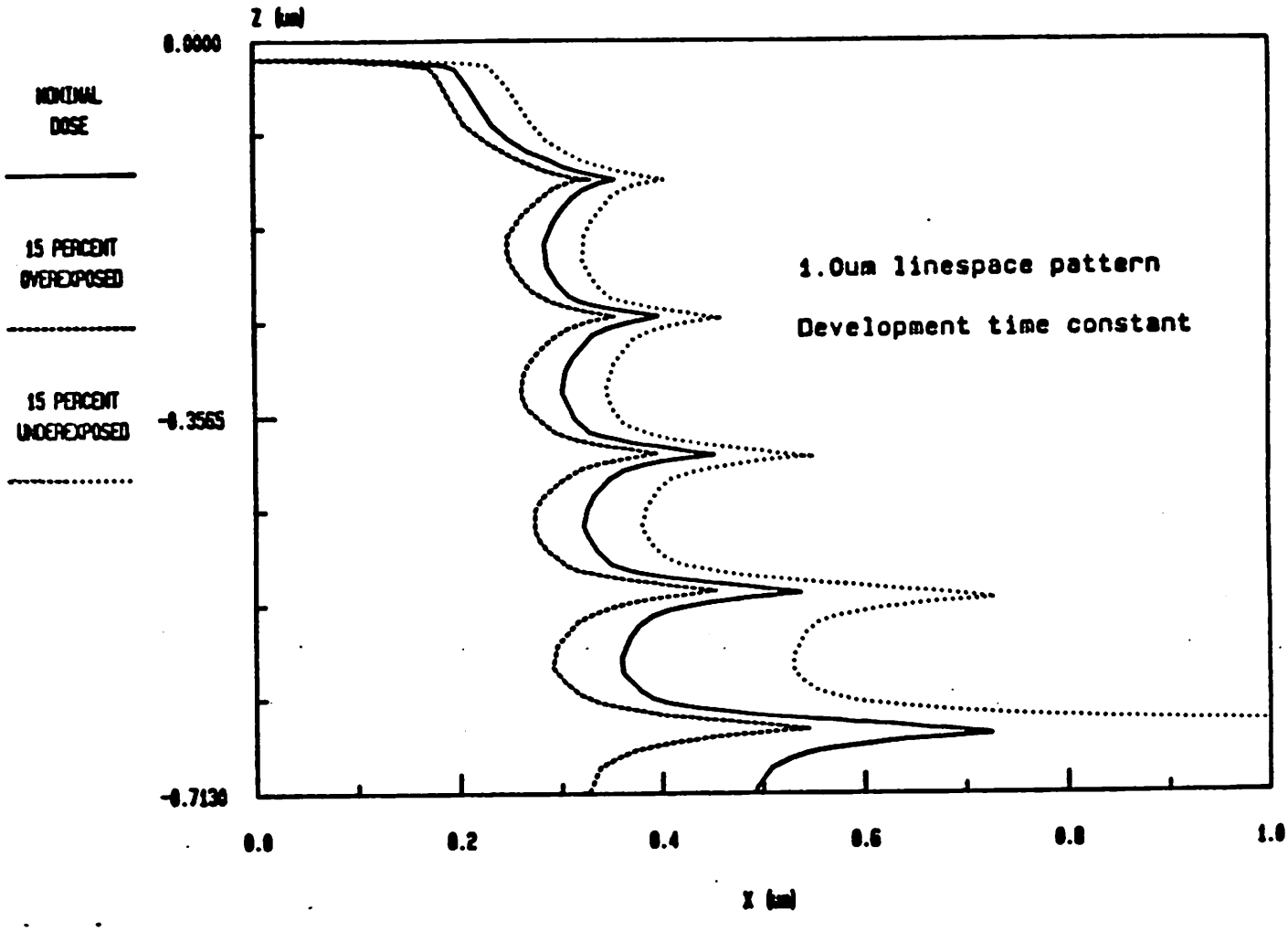

Figure 8. Photoresist development profiles with 15% overexposure and underexposure for a 1.0 μm line and space pattern without CEM.

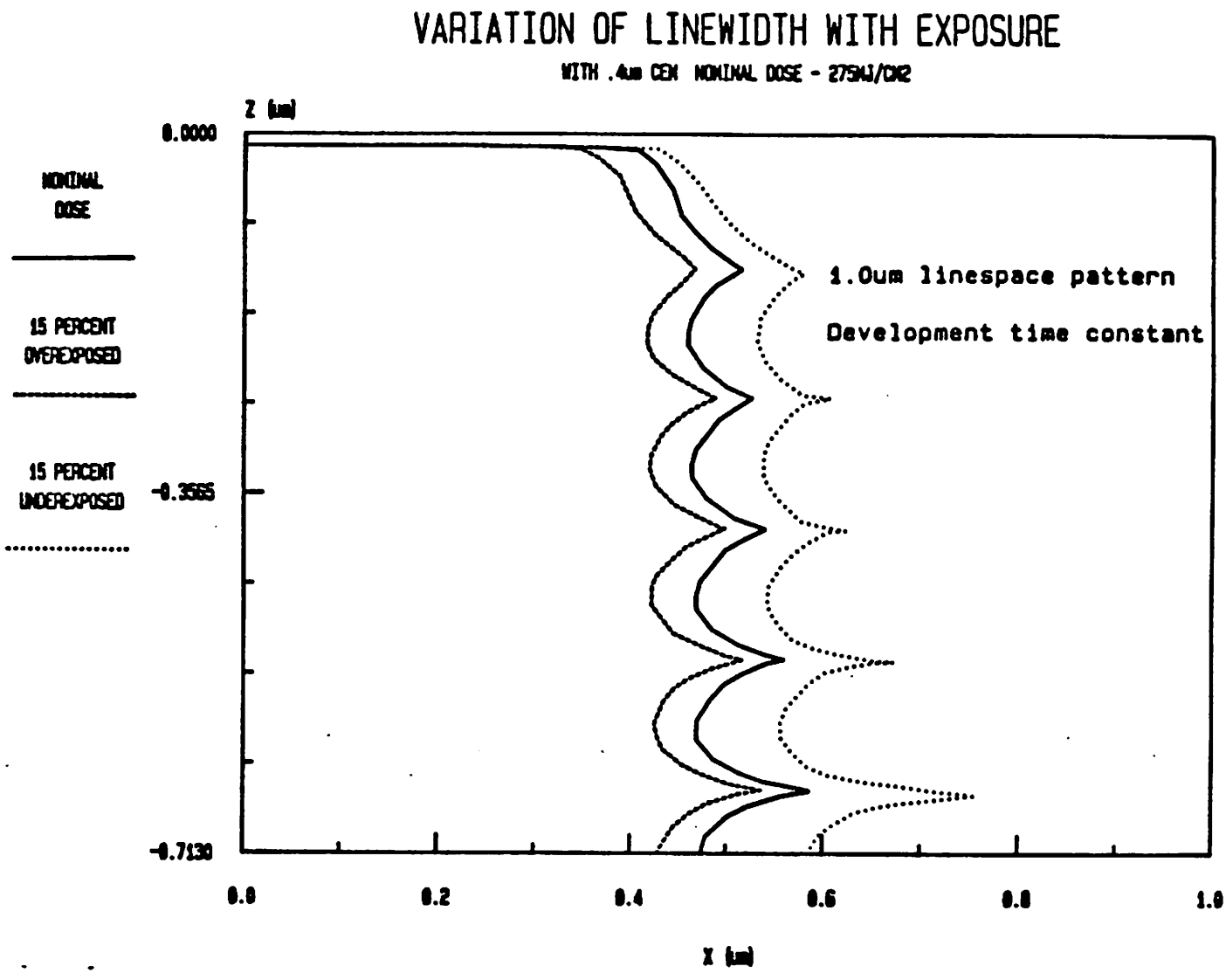

Figure 9. Photoresist development profiles with 15% overexposure and underexposure for a 1.0 μm line and space pattern with CEM.

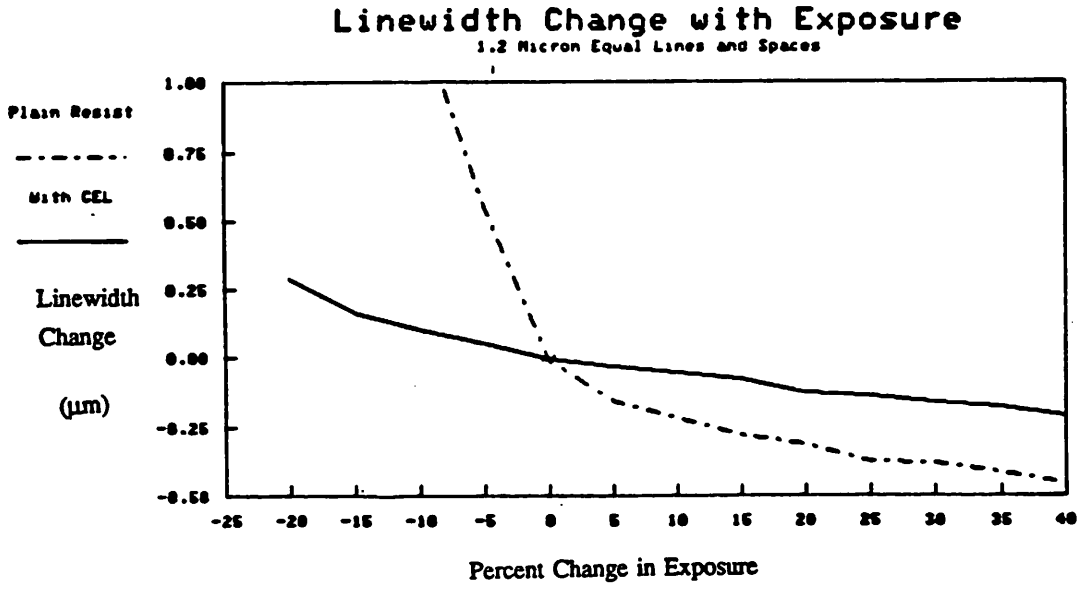

Figure 10. Simulated linewidth change as a function of percent change in exposure. Mask is 1.2 µm line and space pattern. Resist thickness is 1.5 µm.

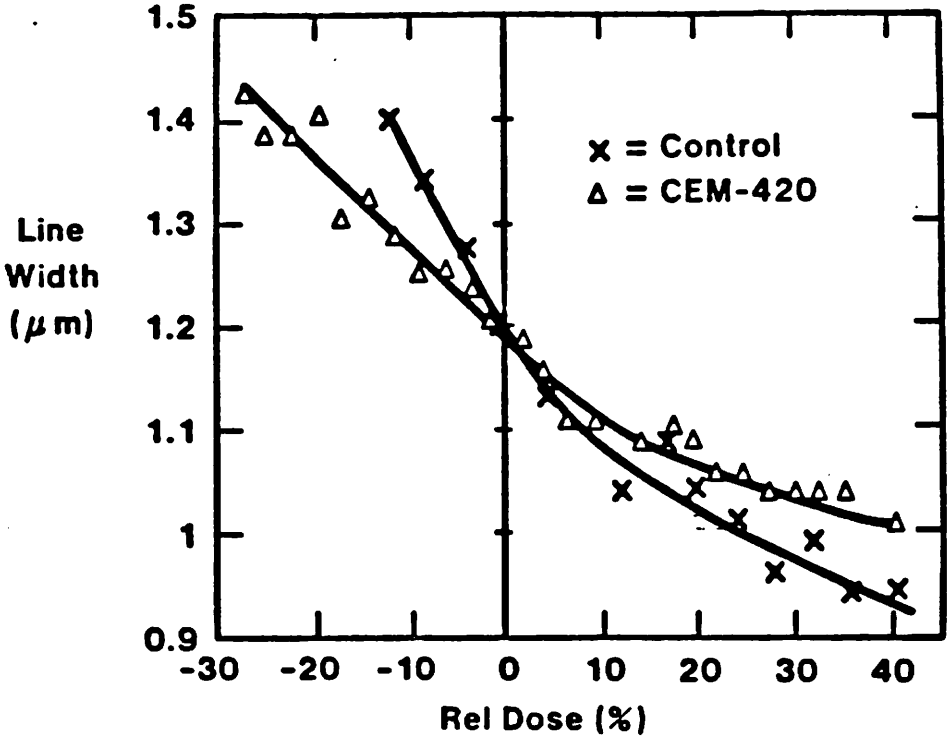

Figure 11. Experimental linewidth change as a function of percent change in exposure. Mask is 1.2 µm line and space pattern. Resist thickness is 1.5 µm.

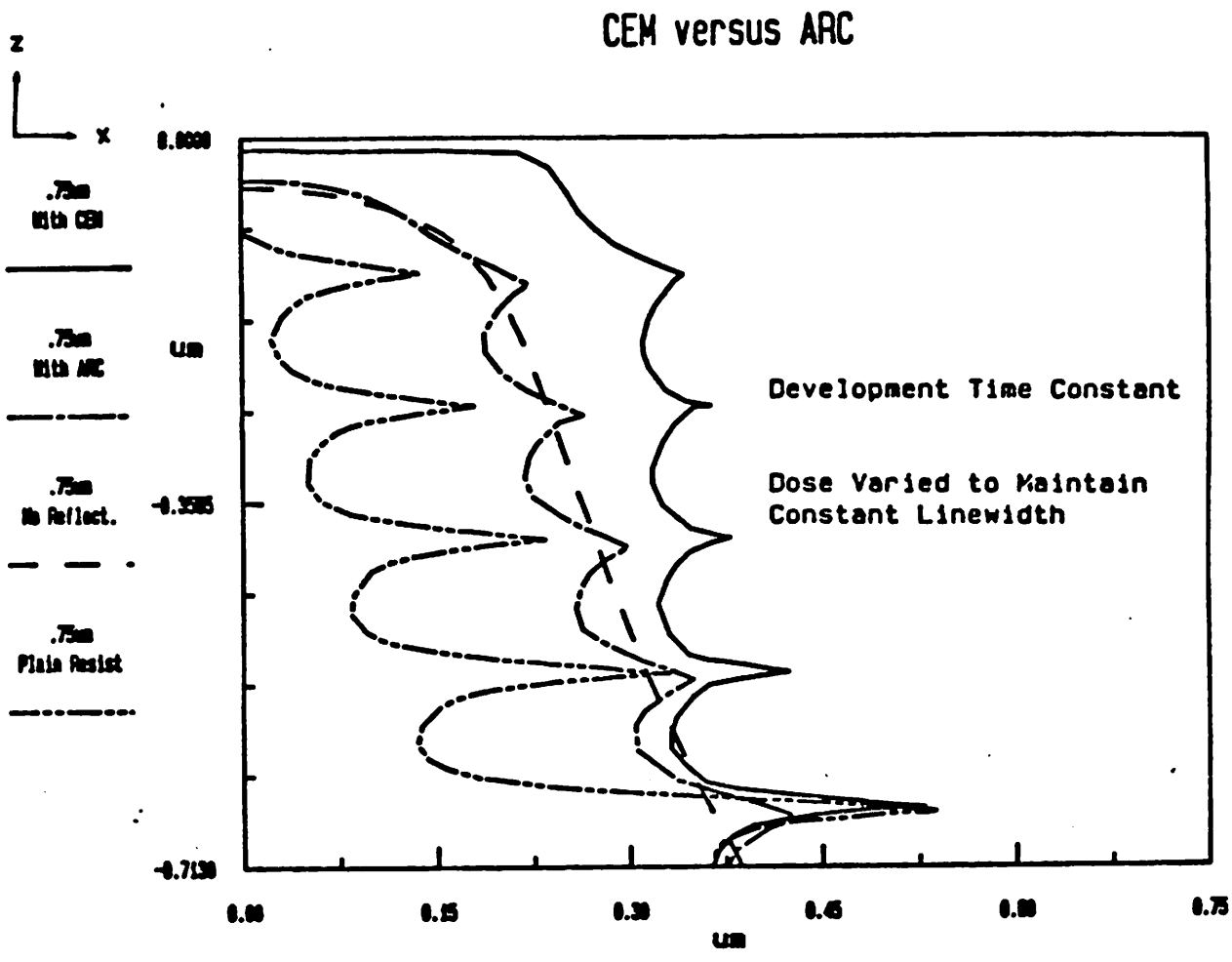

Figure 12. Photoresist development profiles for standard resist, ARC, and CEM processes on a silicon substrate. Mask is 0.75 μm (0.5λ/NA) line and space pattern.

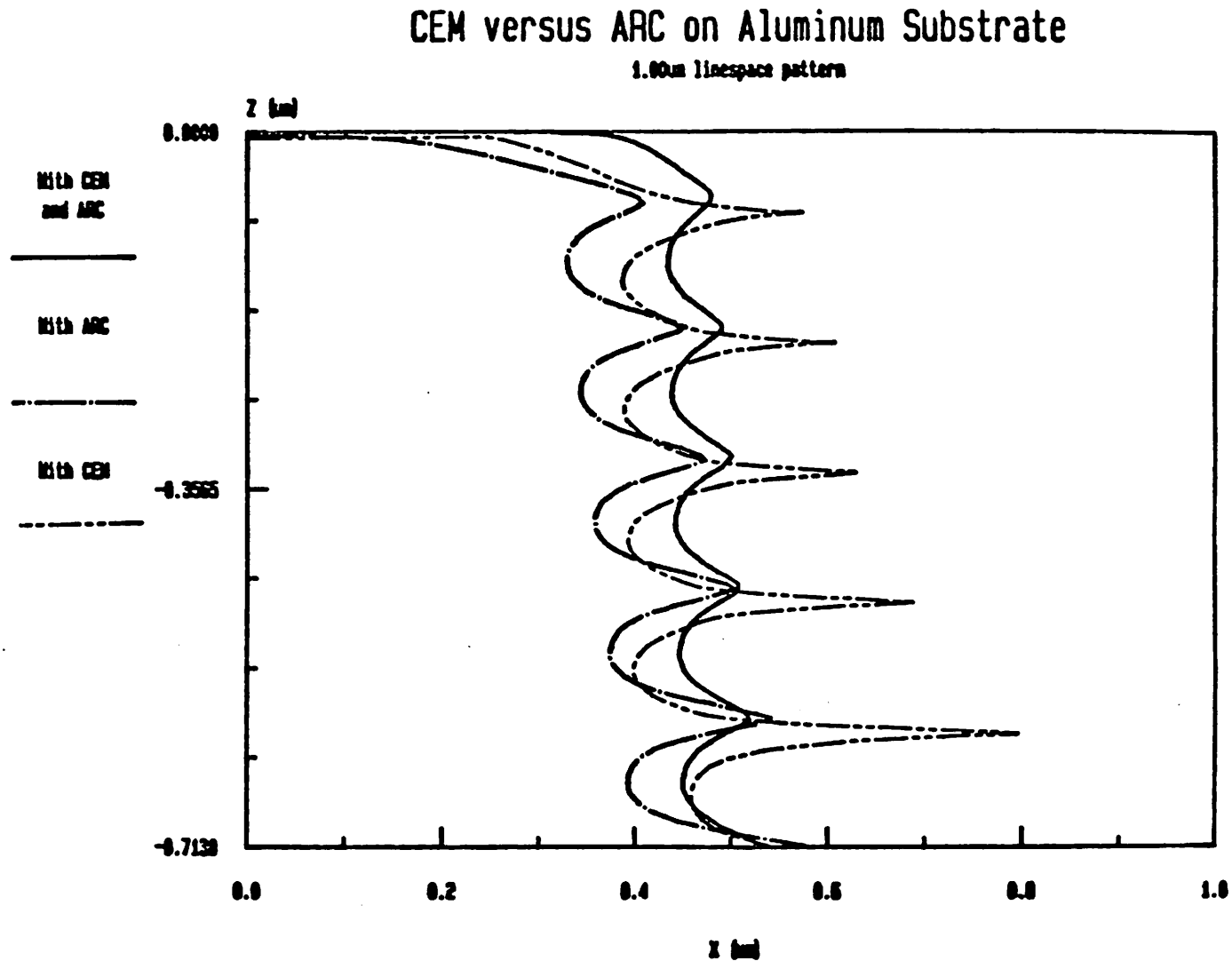

Figure 13. Photoresist development profiles for ARC, CEM, and combined ARC and CEM processes on an aluminum substrate. Mask is 1.0 μm (0.65λ/NA) line and space pattern.

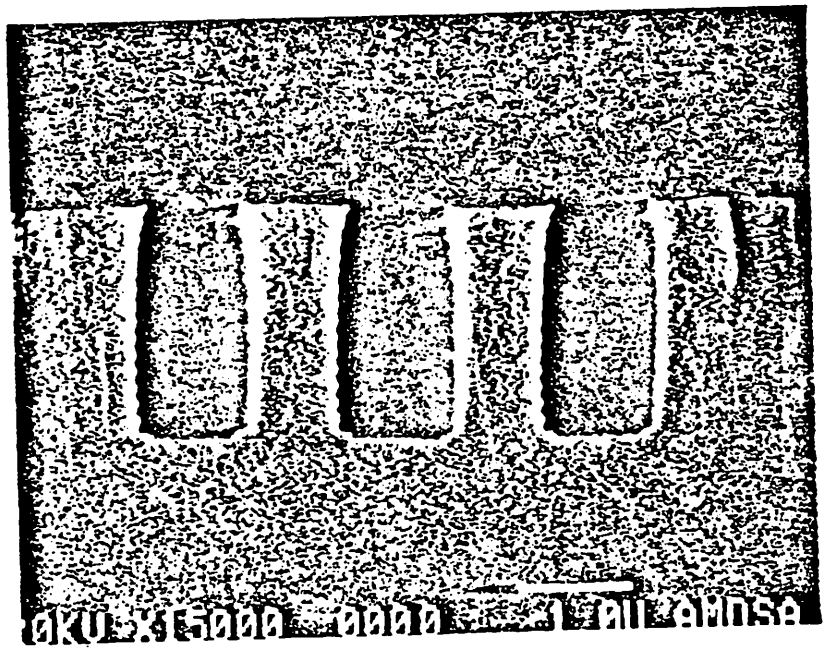

Figure 14. SEM from AMD of photoresist development profile from CEM process. Profile demonstrates a surface induction effect.

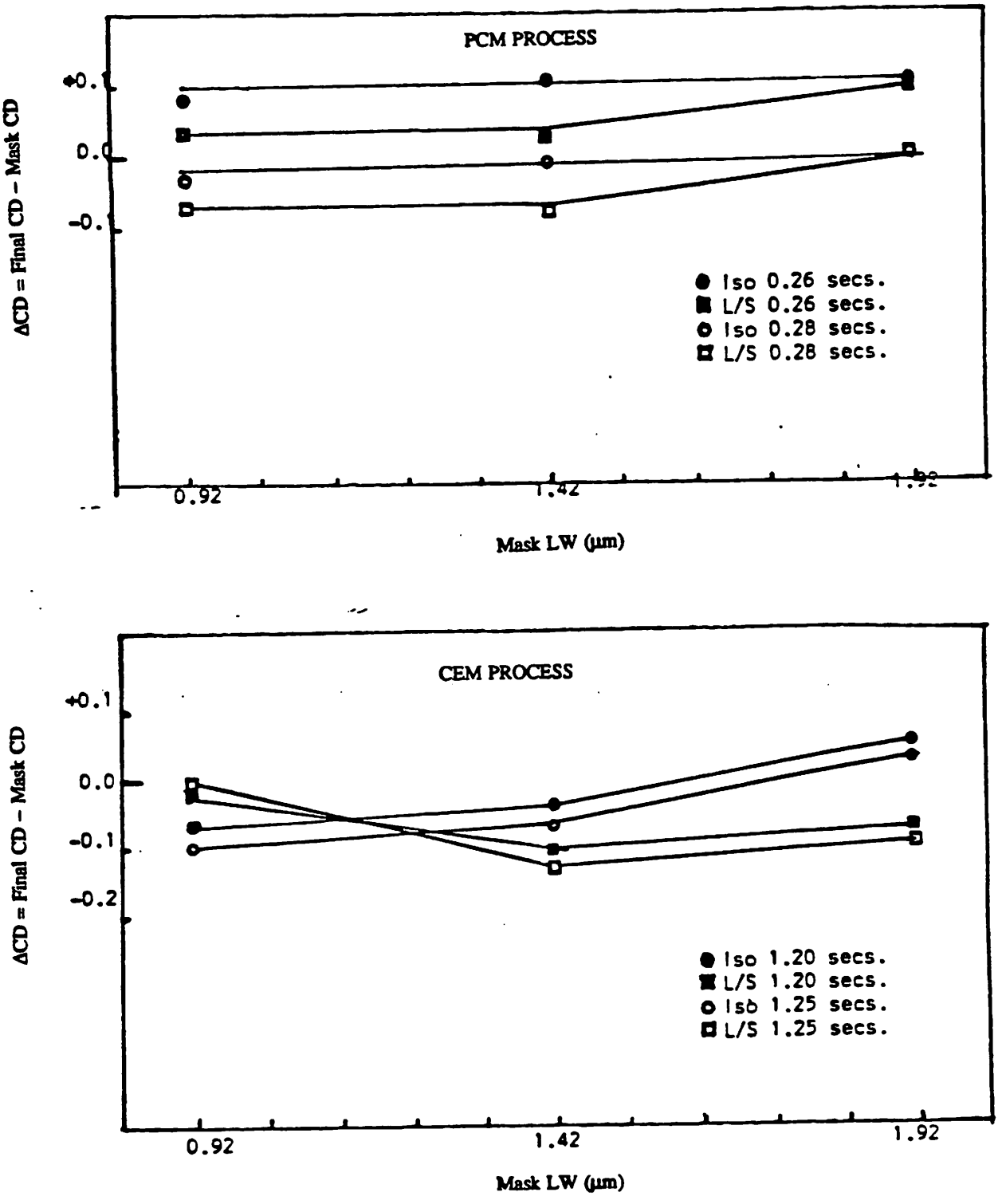

Figure 15. Experimental results on silicon substrates.

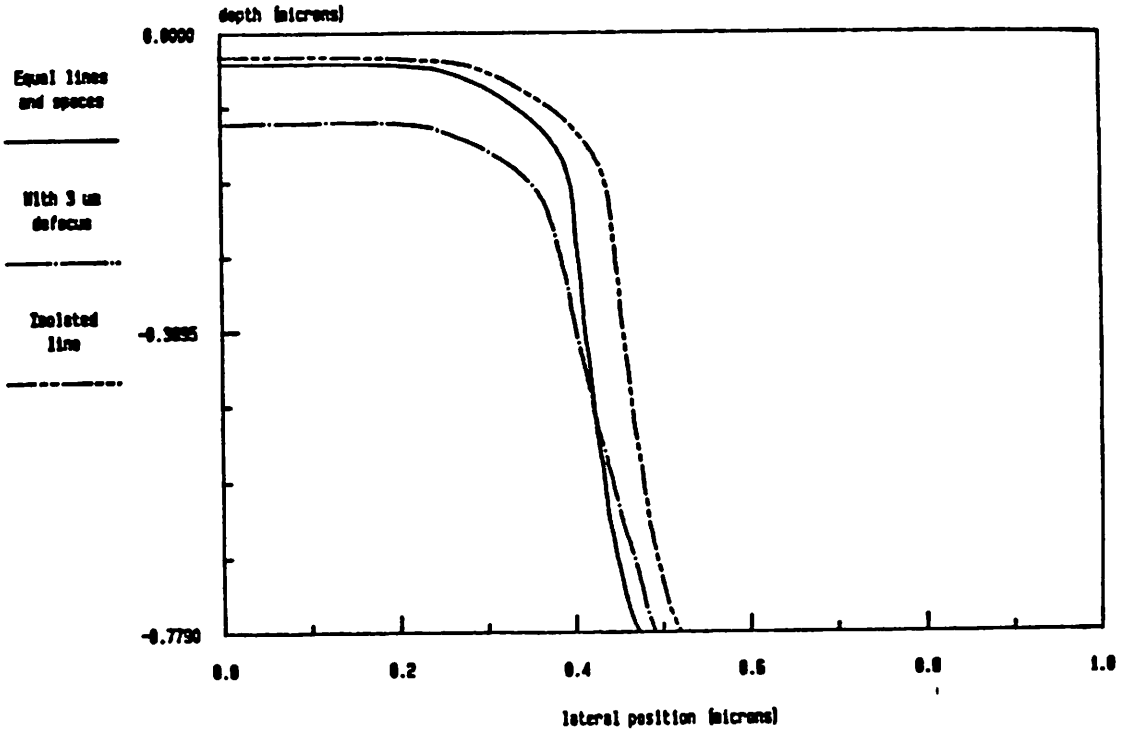

Figure 16. Photoresist development profiles for 1.0 μm features with PCM process.

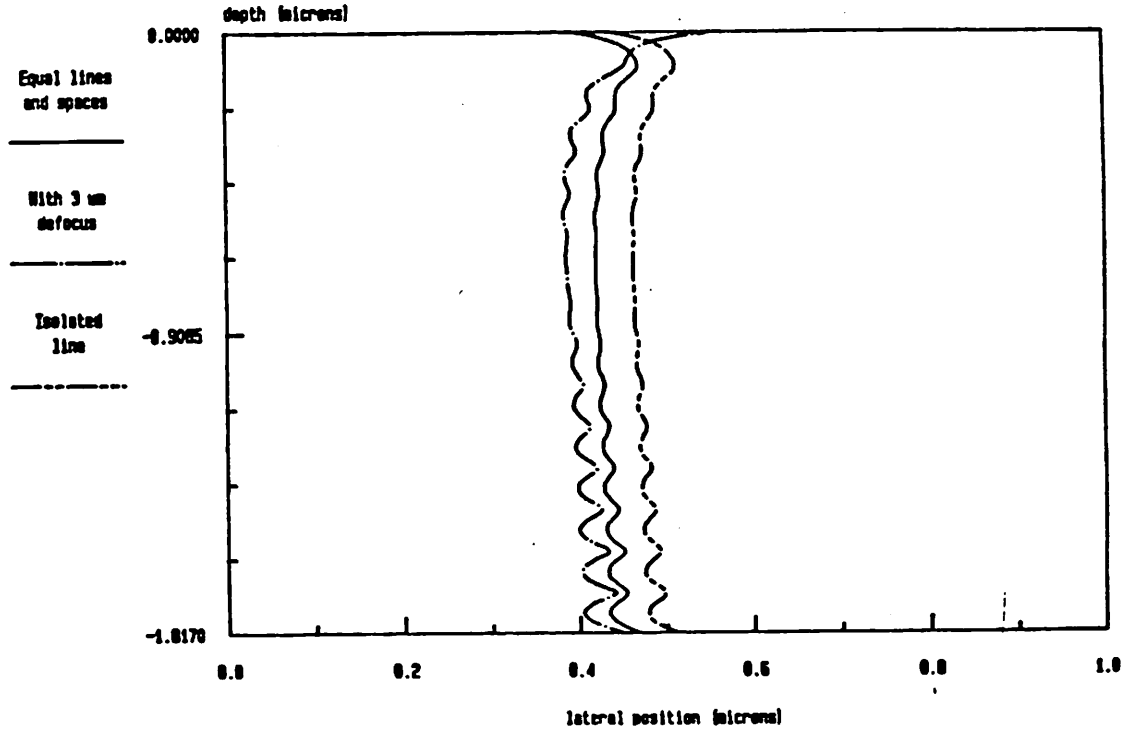

Figure 17. Photoresist development profiles for 1.0 μm features with CEM process on a silicon substrate.

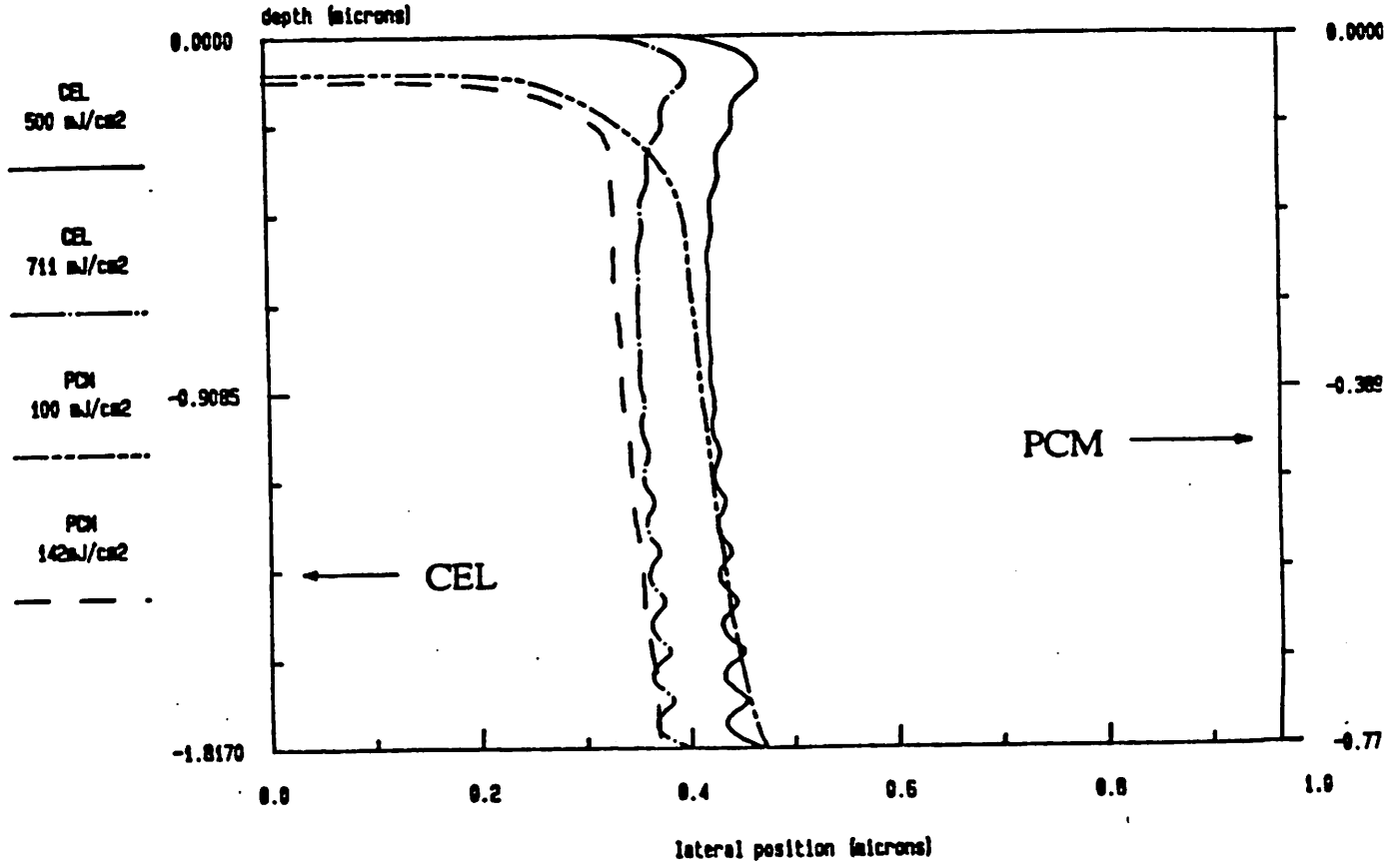

Figure 18. Comparison of linewidth changes with exposure for 1.0 μm features with CEM and PCM processes on a silicon substrate.

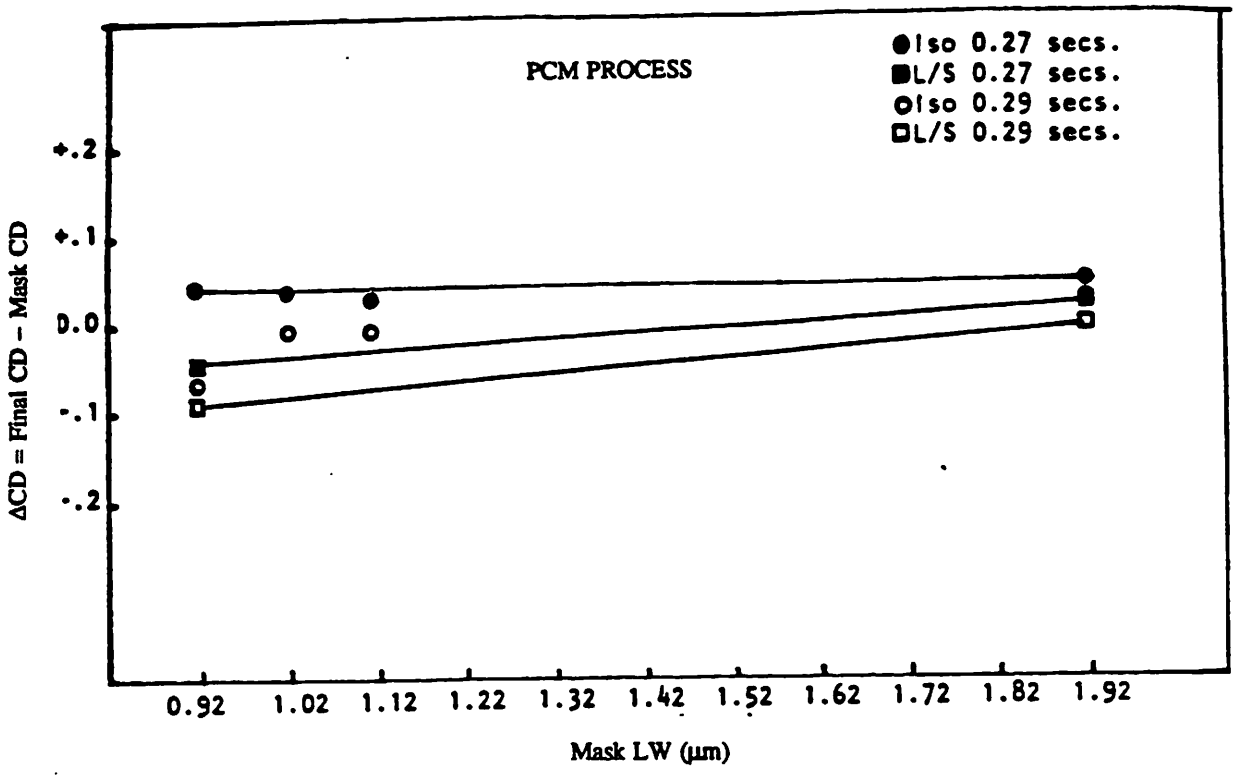

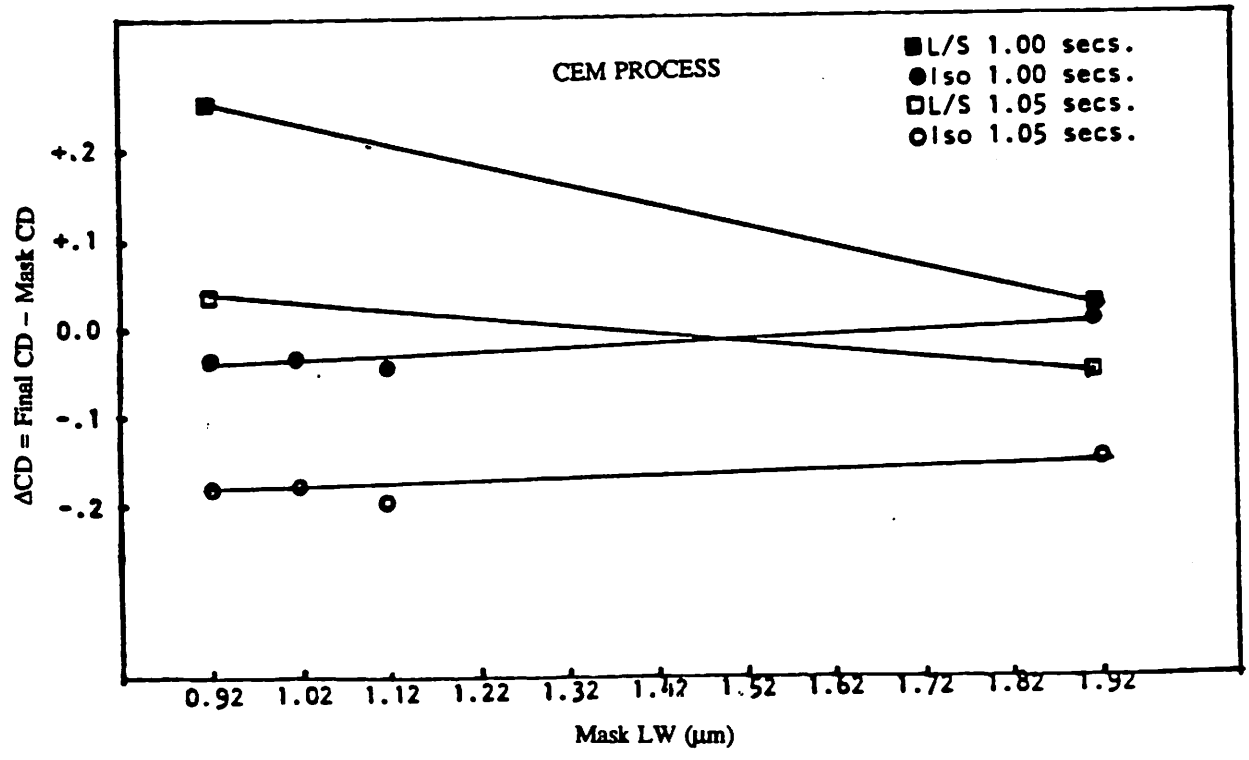

Figure 19. Experimental results on aluminum substrates.

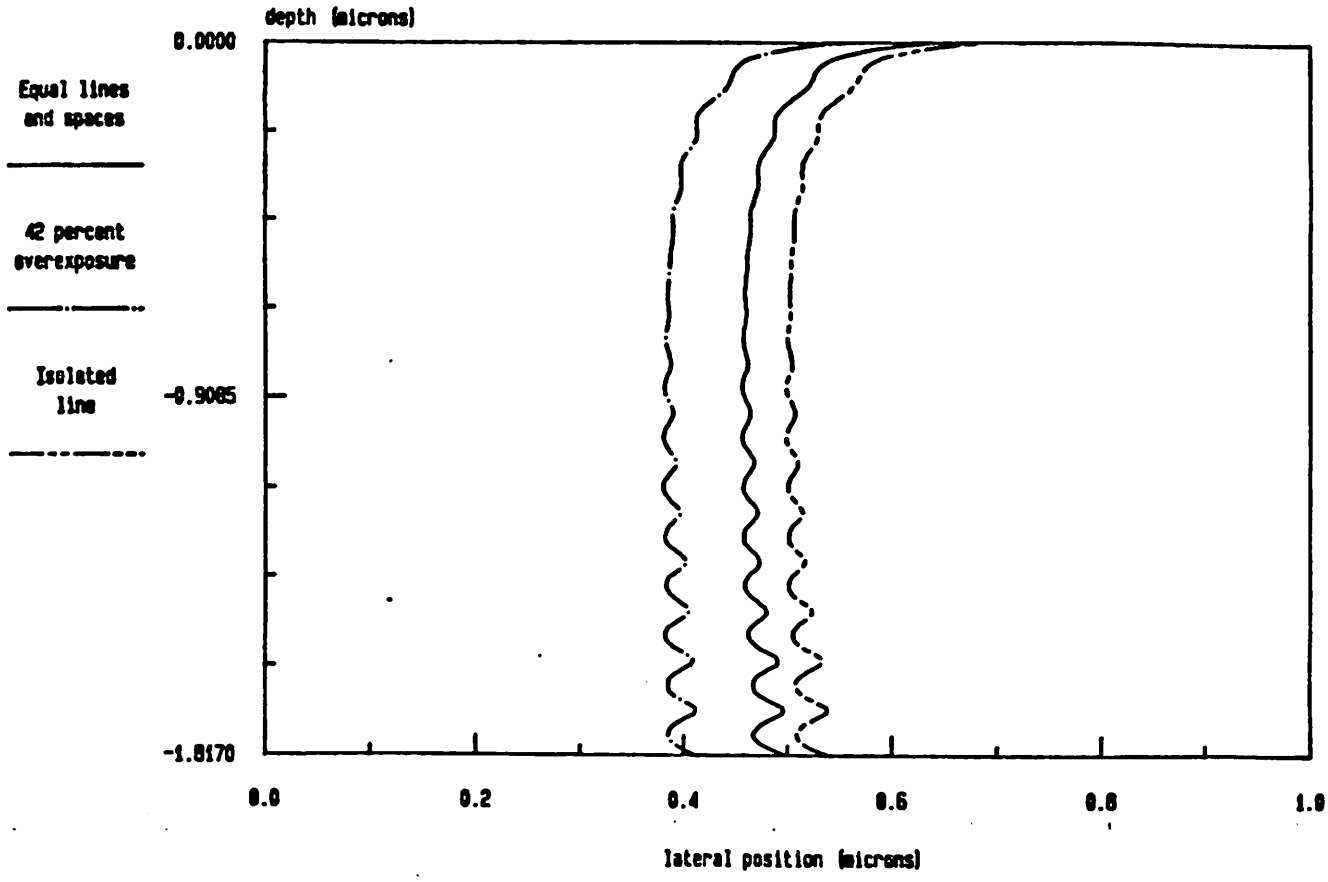

Figure 20. Photoresist development profiles for 1.0 μm features with CEM process on an aluminum substrate.

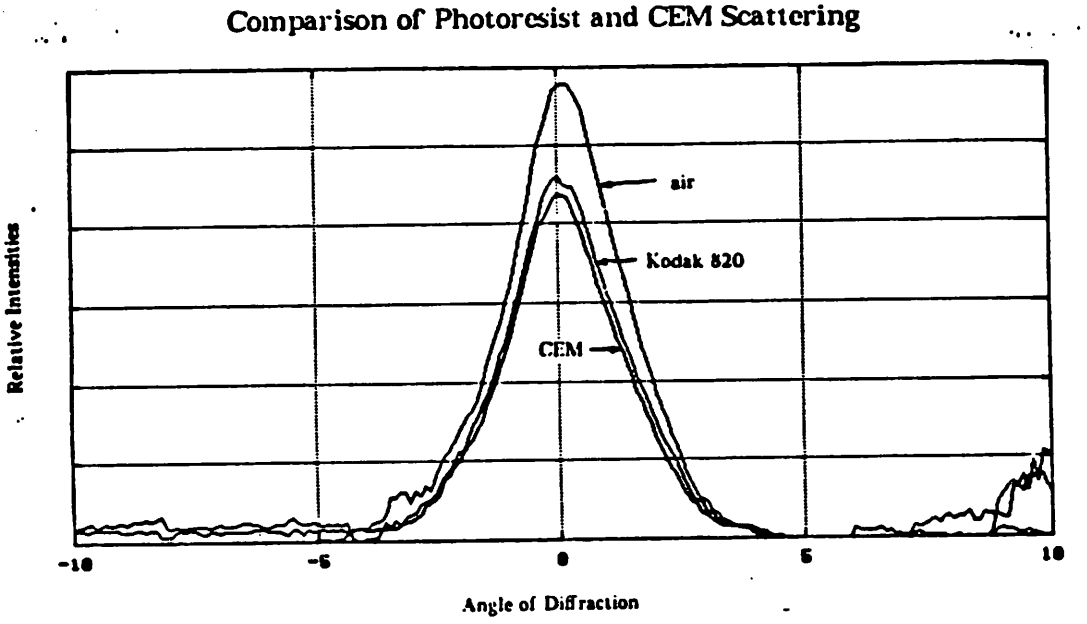

Figure 21. Comparison of scattering in CEM-420 and Kodak 820 photoresist. CEM-420 was 0.6 μm thick and Kodak 820 was 1.3 μm thick. Experiment performed with $\lambda = 633$ nm.

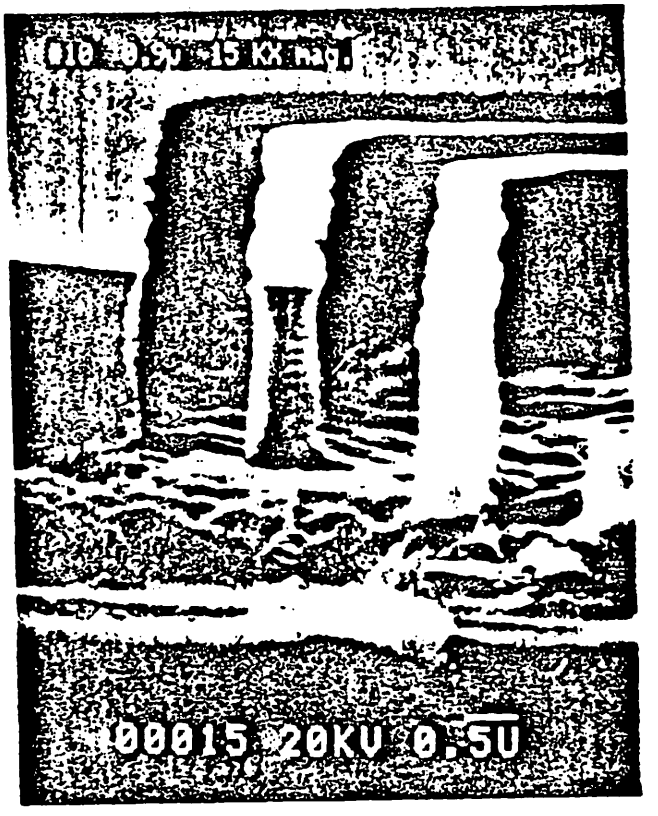

Figure 22. SEM from AMD of photoresist development profile from CEM process on an aluminum substrate. Surface is rough and resist is notched.